HHS Public Access

Author manuscript

Nature. Author manuscript; available in PMC 2014 May 07.

Published in final edited form as:

Nature. 2013 November 7; 503(7474): 131–135. doi:10.1038/nature12613.

A directional switch of integrin signaling and a new anti-thrombotic strategy

Bo Shen, **Xiaojuan Zhao**, **Kelly A. O'Brien**, **Aleksandra Stojanovic-Terpo**, **M. Keegan Delaney**, **Kyungho Kim**, **Jaehyung Cho**, **Stephen C.-T. Lam**, and **Xiaoping Du**

Department of Pharmacology, University of Illinois at Chicago, 835 South Wolcott Ave. Room E403, Chicago, IL 60612, USA

Abstract

Integrins are critical in thrombosis and hemostasis[1]. Antagonists of the platelet integrin $\alpha_{IIb}\beta_3$ are potent anti-thrombotic drugs, but also have the life-threatening adverse effect of bleeding[2,3]. It is thus desirable to develop new antagonists that do not cause bleeding. Integrins transmit signals bidirectionally[4,5]. Inside-out signaling activates integrins via a talin-dependent mechanism[6,7]. Integrin ligation mediates thrombus formation and outside-in signaling[8,9], which requires $G\alpha_{13}$ and greatly expands thrombi. Here we show that $G\alpha_{13}$ and talin bind to mutually exclusive, but distinct sites within the integrin β_3 cytoplasmic domain in opposing waves. The first talin binding wave mediates inside-out signaling and also "ligand-induced integrin activation", but is not required for outside-in signaling. Integrin ligation induces transient talin dissociation and $G\alpha_{13}$ binding to an ExE motif, which selectively mediates outside-in signaling and platelet spreading. The second talin binding wave is associated with clot retraction. An ExE motif-based inhibitor of $G\alpha_{13}$-integrin interaction selectively abolishes outside-in signaling without affecting integrin ligation, and suppresses occlusive arterial thrombosis without affecting bleeding time. Thus, we have discovered a novel mechanism for the directional switch of integrin signaling and, based on this mechanism, we designed a potent new anti-thrombotic that does not cause bleeding.

Integrin signaling involves the binding of several molecules to the cytoplasmic domain of integrin β subunits including talin[6,7], kindlins[10,11], c-Src[12,13], and $G\alpha_{13}$[8] (Fig. 1a). Co-immunoprecipitation of $G\alpha_{13}$ with various β_3 C-terminal truncation mutants suggests that $G\alpha_{13}$ binding involves the β_3 sequence between K^{729} and T^{741} (Fig. 1b, E.D. Fig 2a), but not the kindlin-/c-Src-binding sequences (Fig. 1a, b). Alignment of different β cytoplasmic domains reveals an ExE motif in this region, in which the first and third Glu residues are conserved among most β subunits, but not β_8 (Fig. 1a). The ExE motif-containing β_1, β_2 and

Correspondence to: Xiaoping Du.

Author contributions:

BS performed most experiments, participated in experimental design, data analysis and manuscript writing. XZ, KAO, AS, and MKD each performed a part of experiments and participated in aspects of data analyses and manuscript writing. KK and JC performed laser-induced thrombosis experiments and data analysis, SC-TL provided talin constructs and purified proteins, participated in discussions and data analyses; XD designed and directed the research, analyzed data and wrote the paper.

Competing financial interests

Patent pending. The authors declare no other competing financial interests.

β_3 all bound $G\alpha_{13}$, but not β_8 (Fig. 1c, E.D. Fig 2f). Wild-type (Wt) and E732A mutant β_3 bound to $G\alpha_{13}$, but not E731A, E733A, AAA (Fig. 1d, E.D. Fig 2b), DED or QSE mutants (E.D. Fig 2e), indicating that the first and third Glu within the ExE motif are important for $G\alpha_{13}$ binding. Synthetic peptides containing the EEERA sequence inhibited $G\alpha_{13}$-β_3 interaction (see below), verifying this ExE motif-containing $G\alpha_{13}$ binding site.

The ExE motif is located in a talin-binding region (Fig. 1a)[14,15]. Over-expression of the integrin-binding talin head domain (THD) in $\alpha_{IIb}\beta_3$-expressing cells inhibited $G\alpha_{13}$ co-immunoprecipitation with β_3 (Fig. 1e). Purified recombinant THD and $G\alpha_{13}$ directly competed for binding to purified GST-β_3 cytoplasmic domain fusion protein (GST-β_3CD) (Fig. 1f, g), indicating that $G\alpha_{13}$ and talin are mutually exclusive in binding to β_3. Interestingly, the binding of talin and $G\alpha_{13}$ is regulated temporally during integrin signaling (Fig. 2). The first wave of talin association with $\alpha_{IIb}\beta_3$ occurred following thrombin-stimulated inside-out signaling (Fig. 2a, b) and before the onset of integrin ligation (as indicated by platelet aggregation (Fig. 2c)). Following integrin ligation, however, talin association with $\alpha_{IIb}\beta_3$ was diminished (Fig. 2a, b). The second wave of talin-β_3 association occurred after full platelet aggregation (Fig. 2a-c), the timing of which correlates with clot retraction. Opposite to the waves of talin binding, the $G\alpha_{13}$-β_3 association was even lower than the basal level during inside-out signaling when the first talin binding wave occurred (Fig. 2a, b), but peaked after integrin ligation when the first talin binding wave subsided, and then decreased again during the second talin-binding wave (Fig. 2a, b). Thus, inside-out and various phases of outside-in signaling are associated with coordinated and opposing waves of $G\alpha_{13}$ and talin binding to β_3.

Importantly, an increase in $G\alpha_{13}$ binding to integrin can only be induced when integrin is activated in the presence of fibrinogen, but not by integrin activation alone (E.D. Fig 3a). Conversely, the integrin inhibitors RGDS (Fig. 2a, b) or EDTA (E.D. Fig 3b, c) prevented dissociation of talin from β_3 and inhibited $G\alpha_{13}$-β_3 interaction in thrombin-stimulated platelets. Thus, the switch from a talin-bound to a $G\alpha_{13}$-bound state of $\alpha_{IIb}\beta_3$ is initiated by the binding of macromolecular ligands.

The opposing waves of talin and $G\alpha_{13}$ binding to β_3 suggest that the interaction of these two proteins with β_3 selectively mediates inside-out and outside-in signaling, respectively. This hypothesis was tested using talin-knockout[16] and shRNA-induced talin-knockdown platelets, which are defective in ADP/fibrinogen-induced, integrin-dependent aggregation (Fig. 2d, e; E.D. Fig 4a, c). Their defective aggregation was fully corrected with manganese or an integrin-activating antibody (LIBS6) (Fig. 2e, E.D. Fig 4c), which activate integrins independently of inside-out signaling. These data confirm a role for talin in inside-out signaling[6,15,17]. It is established that inside-out signaling is not the only pathway of $\alpha_{IIb}\beta_3$ activation. Integrin-fibrinogen interaction may occur independently of inside-out signaling when fibrinogen changes conformation, either by immobilization or conversion to fibrin[18,19]. This is because the initial contact of the exposed ligand recognition sequence, RGD, with resting integrins triggers “ligand-induced integrin activation”[20]. Interestingly, adhesion of resting talin-knockout or -knockdown platelets to immobilized fibrinogen was defective (Fig. 2f, E.D. Fig 4b), indicating the importance of talin in platelet adhesion to immobilized fibrinogen in the absence of inside-out signaling. However, addition of

manganese/integrin-activating antibody fully corrected talin-knockout/knockdown platelet adhesion and spreading (and also the spreading of talin-binding defective mutant β_3-expressing CHO cells[21]) on immobilized fibrinogen (Fig. 2f, g, E.D. Fig 4b, d, e). Thus, the role of talin in resting platelet adhesion to fibrinogen is solely due to its importance in "ligand-induced integrin activation". Because cell spreading requires the early phase of outside-in signaling, these data further demonstrate that talin is not required for the early phase of outside-in signaling leading to cell spreading once its role in integrin activation is bypassed.

To assess whether $G\alpha_{13}$ binding to the ExE motif selectively mediates outside-in signaling without perturbing talin-dependent integrin function, Wt and AAA mutant β_3-transfected bone marrow stem cells (from $\beta_3^{-/-}$ mice) were transplanted into irradiated $\beta_3^{-/-}$ mice. The platelets from the recipient mice expressed similar levels of Wt or AAA mutant β_3 (Fig. 3a, E.D. Fig 5a). The AAA mutation inhibited β_3 interaction with $G\alpha_{13}$, but not talin (nor c-Src) (Fig. 3b, E.D. Fig 5b), during integrin signaling. The AAA mutation also had no effect on agonist-induced soluble fibrinogen binding (Fig. 3c). Thus, the ExE motif is not required for talin-dependent inside-out signaling. In contrast, the AAA mutant β_3-expressing platelets were defective in spreading on immobilized fibrinogen (Fig. 3d, E.D. Fig 5c, d). Thus, $G\alpha_{13}$ binding deficiency in β_3 causes a selective defect in integrin outside-in signaling and platelet spreading. Similarly, α_{IIb}/AAA and more conserved α_{IIb}/DED or α_{IIb}/QSE mutants expressed in CHO cells, all defective in $G\alpha_{13}$ binding (E.D. Fig 2e), were also defective in spreading on fibrinogen (Fig. 3e, f, E.D. Fig 6a, b, c). However, AAA mutant β_3 expressed in CHO cells had no negative effect on THD binding, in contrast to the Y747A mutant (E.D. Fig 6d, e). Additionally, AAA-expressing cells showed defects in integrin-dependent activation of c-Src (as shown by phosphorylation at Tyr^{416}) and transient inhibition of RhoA during cell spreading (Fig. 3g, E.D. Fig 6f), both of which are important elements of outside-in signaling. Together with previous studies that identified β_3 sequences mediating talin binding (Fig. 1a)[6,15,17,22], our data suggest that talin and $G\alpha_{13}$ dynamically interact with distinct recognition sequences in the same region of β_3 to serve as a molecular switch controlling the direction of integrin signaling.

The specific role of the ExE motif in outside-in signaling prompted us to design selective inhibitors of outside-in signaling. We synthesized several myristoylated ExE motif-containing β_3 peptides: mP_5 (Myr-EEERA), mP_6 (Myr-FEEERA) and mP_{13} (Myr-KFEEERARAKWDT). These peptides inhibited co-immunoprecipitation between $G\alpha_{13}$ and β_3 (Fig. 4a, E.D. Fig 7a-d), indicating that the minimal sequence of EEERA is sufficient to bind $G\alpha_{13}$. In contrast, only mP_{13}, but not mP_6 (nor mP_5), inhibited talin association with β_3 (Fig. 4a), indicating that mP_6 does not interact with talin. mP_6 inhibited platelet spreading on fibrinogen (Fig. 4b, E.D. Fig 7e), but had no effect on either agonist-induced fibrinogen/PAC1 binding to platelets (Fig. 4c, E.D. Fig 7f, g) or platelet adhesion to immobilized fibrinogen (Fig. 4d). Interestingly, mP_6 did not inhibit, but rather accelerated, platelet-dependent clot retraction (Fig. 4e). These data indicate that the ExE-based inhibitor, mP_6, selectively inhibits the early phase of outside-in signaling without affecting talin-dependent inside-out signaling, ligand-induced integrin activation, or the late phase of outside-in signaling associated with the second wave of talin binding. In contrast, mP_{13} inhibited inside-out and outside-in signaling, as it inhibited fibrinogen binding (E.D. Fig 7h), platelet

adhesion (Fig. 4d) and clot retraction (Fig. 4e) (not reversed by manganese, as previously shown using talin$^{-/-}$ platelets[16]). Thus, mP_6 selectively interferes with the early phase of outside-in signaling, but mP_{13} affects all phases of integrin signaling. Importantly, mP_6 inhibited the second wave of thrombin-induced platelet aggregation *in vitro* (Fig. 4f), and when injected into mice as micelles, was as potent as the currently used integrin antagonist Integrilin in inhibiting laser-induced arteriolar thrombosis (Fig. 4g, h, E.D. Fig 8a, b, videos in Supplementary Materials) and $FeCl_3$-induced occlusive carotid artery thrombosis (Fig. 4i, E.D. Fig 8c). More strikingly, at the concentration in which both Integrilin and mP_6 similarly inhibited occlusive thrombosis, Integrilin dramatically prolonged tail bleeding and increased blood loss, whereas mP_6 had no such adverse effect (Fig. 4j, E.D. Fig 8d). Thus, we have discovered a novel anti-thrombotic that prevents thrombosis without causing bleeding.

Together, our study provides a conceptual advance by revealing a molecular switch controlling the directions and consequences of integrin signaling. We show that the switch between inside-out and outside-in signaling is mediated by coordinated but opposing waves of talin and $G\alpha_{13}$ binding to distinct yet adjacent sequences within the β_3 cytoplasmic domain. The discovery of this signaling switch forms a conceptual basis for selectively inhibiting outside-in signaling without perturbing the ligand binding function of integrins. Importantly, we translated this new concept into a potent novel anti-thrombotic, which, unlike currently available integrin antagonists or other anti-thrombotics, potently inhibits arterial thrombosis without the adverse effect of bleeding (Fig. 4g-j), a potentially life-threatening problem that limits the clinical use of current anti-integrin and anti-thrombotic therapies.

Online only methods

Animals and Reagents

Integrin $\beta_3^{-/-}$ mice were obtained from the Jackson Laboratory. Talin-$1^{(fl/fl)}$, PF4-Cre mice were kindly provided by Dr. Brian Petrich and Dr. David Critchley[16]. Animal usage and protocol were approved by the institutional animal care committee of the University of Illinois at Chicago. For all animal experiments, mice with similar age, weight, and sex ratio (1:1, except for laser-induced thrombosis) were used for control and specific treatment. The individual mice chosen for specific treatment were decided randomly. Human integrin β_3 cDNA was cloned into pcDNA3.1 vector following digestion with Hind III and Xho I, or pLenti6-V5/Dest vector following digestion with EcoR I, Mfe I, and Xho I. Truncation mutants and integrin E to A mutants were either previously reported[23] or generated using PCR and cloned into pcDNA3.1 vector by Bam HI and Xho I. The primer sequences used are: (1): $ITGB_3$-UP: 5'-GCGAAGCTTGCCGCCATGGACCGAGCGCGGCCGCGGCCCCGGCCGCTCT-3'; (2): $ITGB_3$-728DN: 5'-GCGCTCGAGTCAAGCGAATTCTTTTCGGTCGTGGATGGTGATGAG-3'; (3): $ITGB_3$-715DN: 5'-GCGCTCGAGTCACCAGATGAGCAGGGCGGCAAGGCCAATGAGCAG-3'; (4): $Itgb_3$-E731A-up: 5'-AAGAATTCGCTAAATTTGCAGAAGAACGCGCCAGAGCAA-3'; (5):

Itgb$_3$-E732A-up: 5'-AAGAATTCGCTAAATTTGAGGCAGAACGCGCCAGAGCAA-3'; (6): Itgb$_3$-E733A-up: 5'-AAGAATTCGCTAAATTTGAGGAAGCACGCGCCAGAGCAA-3'; (7): Itgb$_3$-E731-733A-up: 5'-AAGAATTCGCTAAATTTGCAGCAGCACGCGCCAGAGCAA-3'; (8): Mfe-ITGB$_3$-Up: 5'-CCGCAATTGGCCGCCATGGACCGAGCGCGGCCGCGGCCCCGGCCGCTCT-3'; (9): Xho I-ITGB$_3$-DN: 5'- GCGCTCGAGTTAAGTGCCCCGGTACGTGATATTG-3'. Human integrin β_8-CD cDNA was cloned into pGEX4T-1 vector following digestion with Bam HI and Xho I. Primer sequences used are: (1): ITGB$_8$-UP: 5'- CGTGGATCC ATTAGACAGGTGATACTACAATGG -3'; (2): ITGB$_8$-Dn: 5'- GCGCTCGAGTTAGA AGTTGCACCTGAAAGTTTC -3'. GST-β_3CD and recombinant Gα_{13} purification was described previously[8]. Human talin head domain (THD) cDNA, corresponding to N-terminal talin amino acid residues 1-433, was cloned into pcDNA3.1 vector and pMal-C2 vector between EcoR I and Xho I sites. Anti-RhoA antibody was purchased from Cytoskeleton, Inc.; anti-Gα_{13}(sc410), anti-c-Src (sc18), anti-talin (sc7534), and anti-integrin β_3 (sc6627) antibodies were from Santa Cruz Biotechnology, Inc.; anti-Gα_{13}(26004) was from NewEast; anti-phospho-Src Y^{416} antibody was obtained from Cell Signaling; anti-talin (TA205) was from Millipore; anti-talin antibody 8d4 (T3287) was obtained from Sigma; PAC1 antibody (340507) and anti-mouse α_{IIb} antibody MWReg3 (14-0411) were obtained from BD Biosciences; anti-human integrin β_3 antibody MAb15, LIBS6 and 8053 rabbit serum were kindly provided by Dr. Mark Ginsberg (University of California, San Diego, La Jolla, CA); Lipofectamine 2000, viraPower lentivirus expression system, Alexa Fluor 546-conjugated phalloidin, Fluor 488-conjugated anti-mouse secondary antibody, talin-1 shRNA plasmids (NM-011602), and non-specific shRNA control vector were from Invitrogen; Y-27632 is from Calbiochem; Fibrinogen from Enzyme Research Laboratories.

Purified Gα_{13} and THD binding to integrin cytoplasmic domains

GST-tagged integrin cytoplasmic domain proteins were coated onto Pierce Glutathione-coated plates (15140) overnight at 4°C. After washing twice with NP40 buffer (50 mM Tris, pH 7.4, 10 mM $MgCl_2$, 150 mM NaCl, 1% NP-40, 1 mM sodium orthovanadate, 1 mM NaF) with complete protease inhibitor cocktail tablets (1 tablet/5 ml buffer, Roche), purified THD or Gα_{13} proteins were added onto the plate in NP40 buffer (for Gα_{13} binding, buffer contained 30 μM AlF_4^-). Bound THD or Gα_{13} was estimated with anti-talin or anti-Gα_{13} antibody, horse radish peroxide (HRP)-conjugated secondary antibody, and 3,3',5,5'-Tetramethylbenzidine Substrates (Pierce, 34021). The wells were washed three times with NP40 buffer between each of these steps. The reactions were terminated with 1 M sulphuric acid and measured for OD_{450}. For the competitive inhibition assay, increasing concentrations of THD or Gα_{13} was added to the reactions.

Platelet preparation

Studies using human blood were approved by the institutional review board at the University of Illinois at Chicago, and informed consent was obtained from all donors. Washed human platelets from healthy donors who have not taken medication within 2 weeks prior to donation and platelets from 8-12 week-old mice were prepared as previously described and resuspended in modified Tyrode's buffer[13].

Platelet aggregation assay

Platelet aggregation and secretion were measured in a turbidometric platelet aggregometer (Chronolog) at 37°C with stirring (1000 rpm). Washed platelets (3×10^8/ml) in modified Tyrode's buffer were stimulated with thrombin (Enzyme Research Laboratories). Aggregation traces shown are representative of at least three independent experiments.

Fibrinogen and PAC1 binding assay

For the fibrinogen binding assay, washed human or mouse platelets resuspended in modified Tyrode's buffer were incubated with 10 μg/ml Oregon Green-conjugated fibrinogen (Molecular Probes) and PAR4AP as described previously[23]. The reaction was diluted with PBS and analyzed by flow cytometry using an Accuri C6 flow cytometry (BD). PAC1 binding was measured with FITC-labelled PAC1 antibody (Molecular Probe).

Co-immunoprecipitation

As previously described[8], platelets or CHO-1b9 cells expressing recombinant integrin $\alpha_{IIb}\beta_3$[23] were solubilized in NP40 lysis buffer (50 mM Tris, pH 7.4, 10 mM $MgCl_2$, 150 mM NaCl, 1% NP-40, 1 mM sodium orthovanadate, 1 mM NaF), with complete protease inhibitor cocktail tablets (1 tablet/5 ml buffer, Roche). Lysis debris was cleared after centrifugation at 14,000g for 10 min. Lysates were then immunoprecipitated with rabbit anti-$G\alpha_{13}$ IgG, anti-integrin β_3 rabbit serum or an equal amount of rabbit IgG or pre-immune serum for 2 hours before Protein A/G sepharose beads were added. After incubation of Protein A/G sepharose beads for 45min at 4 °C, beads were centrifuged down and washed for six times with NP40 lysis buffer. Immunoprecipitates were analyzed by immunoblotting.

RhoA activity assay

Platelets or $\alpha_{IIb}\beta_3$-expressing CHO cells in modified Tyrode's buffer or adherent on immobilized fibrinogen were solubilized in cold NP40 lysis buffer at 4°C, and debris-cleared lysates were incubated for 1 hour with purified GST-RBD beads, washed, and then immunoblotted with an anti-RhoA monoclonal antibody, as previously described[8].

Bone marrow transplantation

As previously described[8], bone marrow stem cells were isolated from femur and tibias of 6-8 week old integrin $\beta_3^{-/-}$, or C57/BL6 mice using the MACS lineage cell depletion kit (Miltenyi Biotec). Stem cells were subsequently infected twice with concentrated lenti-virus containing shRNA or cDNA constructs, as described in Animals and Reagents section, using a Lenti-X concentrator (Clontech). The cells were then retro-orbitally injected into irradiated recipient mice (5Gy for integrin $\beta_3^{-/-}$ mice and 9.6Gy for C57/BL6 mice, one million cells per recipient mice) one day after irradiation.

Platelet Adhesion Assay

As previously described[23], washed platelets were pre-incubated with vehicle or peptides, or with either 1 mM $MnCl_2$ or 0.18 μg/ml LIBS6 prior to plating. After 1 hour incubation at 37°C, adherent platelets were estimated by measuring platelet phosphatase activity with 0.3% *p*-nitrophenyl phosphate in 1% Triton X-100, 50 mM sodium acetate, pH 5.0 for 1

hour at 37°C. The reaction was stopped with 1 M NaOH. Results were determined by reading OD_{405}. Statistic significance was determined using *t*-test (n=3).

Cell spreading, immunofluorescence and confocal microscopy

Washed platelets or $\alpha_{IIb}\beta_3$-expressing CHO cells suspended in modified Tyrode's buffer were added to 100 μg/ml fibrinogen (Enzyme Research Laboratories)-coated cover slides and incubated at 37°C for various lengths of time. Cells were fixed, permeabilized, blocked with 0.5% bovine serum albumin in modified Tyrode's buffer, stained with mAb15 (followed by Fluor 488-conjugated anti-mouse secondary antibody) and/or Alexa Fluor-546 conjugated phalloidin, and viewed with a Zeiss LSM510 META confocal microscope, as previously described[8] or with Leica DM IRB fluorescence microscope, Photometrics CoolSNAP HQ camera and μManager software. Cell surface area was measured by NIH ImageJ analysis of 5-10 random images. Statistical significance was determined using *t*-test.

Clot Retraction Assay

As previously described[8], human PRP was incubated with vehicle or peptides for 5 minutes at room temperature prior to stimulation with thrombin. The two-dimensional size of retracted clots was quantified using Image J software, and statistical significance was determined using *t*-test (n=3).

Peptide inhibitors

Myristoylated peptides were synthesized and purified at the Research Resource Center at the University of Illinois at Chicago. These peptides include: mP_{13} (Myr-KFEEERARAKWDT), mP_5 (Myr-EEERA), mP_6 (Myr-FEEERA), and the corresponding control peptides mP_{13}Scr (Myr-EEARERKDWAKFT), mP_5Scr (Myr-EEARE), and mP_6Scr (Myr-ERAFEE). The peptides were prepared in DMSO for use *in vitro*, and in micellar formulation for *in vivo* (and *in vitro*) use. For micellar formulation, PEG_{2000}-DSPE, L-α-phosphatidylcholine, and peptides were mixed at a molar ratio of 45:5:2. The micelles were suspended to form micelle colloid in HEPES-saline buffer (10 mM HEPES, 150 mM NaCl, pH 7.4), peptide concentration 1 mM) as previously described[24]. mP_6 is similar to mP_6Scr in uptake by platelets (E.D. Fig 9a) and does not cause significant changes in hemogram *in vivo* (E.D. Fig 9b).

Estimation of peptide concentration in platelets

mP_6 and mP_6Scr peptides were dissolved and conjugated with 1-Pyrenyldiazomethane (PDAM) overnight in the dark in DMSO, or conjugated in methanol and incorporated into the micelle as described above. Platelets were incubated with the PDAM-conjugated peptides for 5 minutes at room temperature, pelleted via centrifugation, washed and lysed with NP40 lysis buffer, and the concentration of PDAM-conjugated peptide was estimated by measuring fluorescence intensity (absorption 340 nm/emission 395 nm) as previously described[30]. Platelet lysates (without peptide incubation) were used as a blank control. Standard curve was obtained using known concentrations of peptides added to platelet lysates.

In vivo $FeCl_3$-induced thrombosis and tail bleeding time

7-8 week-old C57/BL6 mice were anesthetized by isoflurane inhalation. Retro-orbital injection of peptide micelle or integrilin (5 μmol/kg mouse weight) were performed 15 minutes prior to experimentation. Carotid arterial thrombosis was induced with a filter paper disc (d = 2 mm) soaked with 1.2 μl of 7.5% $FeCl_3$ [28]. Blood flow was monitored with a TS420 flow meter using a MA-0.5SB dopler probe (Transonic Systems, Ithaca, NY). Data were analyzed using one-way ANOVA. Tail bleeding time analysis were performed as previously described[29]. Time to stable cessation of bleeding was defined as no evidence of rebleeding for 60 seconds. Bleeding exceeding 15 minutes was immediately stopped by applying pressure. Statistical significance was determined using the Mann-Whitney test. Similar results were also obtained with a nonparametric ANOVA. For bleeding assays measuring total blood loss, cut mouse tails were immersed in Microcentrifuge tubes with 1.5 ml of 0.15 M NaCl at 37 °C for 15 minutes. The hemoglobin concentration in the tube was determined using a HemoCue photometer. Data were analyzed using one-way ANOVA. The experiments were performed in double-blinded fashion.

Intravital Microscopy and Laser-induced thrombosis

Similar to the methods described previously[27], Wt male mice (6-8 weeks old) were anesthetized via IP injection of ketamine and xylazine and placed on a thermo-controlled blanket (37°C). The cremaster muscle was exteriorized and superfused with thermo-controlled (37°C) bicarbonate-buffered saline for the duration of experiments. Fluorescence and brightfield images were recorded using an Olympus BX61W microscope with a 60 x/1.0 NA water immersion objective and a high speed camera (Hamamatsu C9300) through an intensifier (Video Scope International). Fluorescence images were captured at 20 frames per second, and data were analyzed using Slidebook v5.5 (Intelligent Imaging Innovations). Arteriolar wall injury was induced with a micropoint laser ablation system (Photonics Instruments). Platelet accumulation was visualized by infusion of Dylight 649-labeled anti-mouse CD42c (Emfret, 0.05 μg/g body weight body weight) into mice. Vehicle control, Integrilin, scrambled peptide, or mP_6 were infused 3 minutes prior to laser injury. Laser-induced thrombi were generated at different sites in the blood vessel, with new sites upstream of earlier thrombi. Data were collected for 5 minutes following laser injury. The kinetics of platelet accumulation was analyzed by median fluorescence values of the antibodies as a function of time in approximately 30 thrombi in 3 mice per group. Statistical difference of fluorescence intensity (mean ± SD) at selected time points was also determined using Welch *t*-test. The experiments were performed in double-blinded fashion.

Statistics

For parametric data, statistical significance was analysed using Student's *t*-test (or Welch *t*-test for samples with nonequal variances) or ANOVA following determination of normal distribution and equal variances. For nonparametric data (bleeding time analysis), Mann-Whitney test was applied. Analyses were performed with GraphPad Prism 4 software. Sample size estimation was performed with Fisher's exact test using GraphPad InStat 3.

Supplementary Material

Refer to Web version on PubMed Central for supplementary material.

Acknowledgments

We thank Drs. Tohru Kozasa, Barry Kreutz and Christina Chow for providing purified recombinant $G\alpha_{13}$ protein; Drs. Brian Petrich and David Critchley for providing talin$^{-/-}$ mice. We acknowledge that Haixia Gong performed experiments for this project. This work is supported by grants from National Heart, Lung and Blood Institute (HL080264, HL062350 (X.D.), and HL109439 (J.C)).

References

1. Shattil SJ, Newman PJ. Integrins: dynamic scaffolds for adhesion and signaling in platelets. Blood. 2004; 104:1606–1615. [PubMed: 15205259]
2. Coller BS. Anti-GPIIb/IIIa drugs: current strategies and future directions. Thromb Haemost. 2001; 86:427–443. [PubMed: 11487034]
3. Serebruany VL, Malinin AI, Eisert RM, Sane DC. Risk of bleeding complications with antiplatelet agents: meta-analysis of 338,191 patients enrolled in 50 randomized controlled trials. American journal of hematology. 2004; 75:40–47. [PubMed: 14695631]
4. Hynes RO. Integrins: bidirectional, allosteric signaling machines. Cell. 2002; 110:673–687. [PubMed: 12297042]
5. Moissoglu K, Schwartz MA. Integrin signalling in directed cell migration. Biol Cell. 2006; 98:547–555. [PubMed: 16907663]
6. Tadokoro S, et al. Talin binding to integrin beta tails: a final common step in integrin activation. Science. 2003; 302:103–106. [PubMed: 14526080]
7. Ye F, Kim C, Ginsberg MH. Molecular mechanism of inside-out integrin regulation. J Thromb Haemost. 2011; 9(Suppl 1):20–25. [PubMed: 21781238]
8. Gong H, et al. G protein subunit Galpha13 binds to integrin alphaIIbbeta3 and mediates integrin “outside-in” signaling. Science. 2010; 327:340–343. [PubMed: 20075254]
9. Shen B, Delaney MK, Du X. Inside-out, outside-in, and inside-outside-in: G protein signaling in integrin-mediated cell adhesion, spreading, and retraction. Current opinion in cell biology. 2012; 24:600–606. [PubMed: 22980731]
10. Moser M, Nieswandt B, Ussar S, Pozgajova M, Fassler R. Kindlin-3 is essential for integrin activation and platelet aggregation. Nat Med. 2008; 14:325–330. [PubMed: 18278053]
11. Ma YQ, Qin J, Wu C, Plow EF. Kindlin-2 (Mig-2): a co-activator of beta3 integrins. J Cell Biol. 2008; 181:439–446. [PubMed: 18458155]
12. Obergfell A, et al. Coordinate interactions of Csk, Src, and Syk kinases with [alpha]IIb[beta]3 initiate integrin signaling to the cytoskeleton. J Cell Biol. 2002; 157:265–275. [PubMed: 11940607]
13. Flevaris P, et al. A molecular switch that controls cell spreading and retraction. J Cell Biol. 2007; 179:553–565. [PubMed: 17967945]
14. Patil S, et al. Identification of a talin-binding site in the integrin beta(3) subunit distinct from the NPLY regulatory motif of post-ligand binding functions. The talin n-terminal head domain interacts with the membrane-proximal region of the beta(3) cytoplasmic tail. J Biol Chem. 1999; 274:28575–28583. [PubMed: 10497223]
15. Wegener KL, et al. Structural basis of integrin activation by talin. Cell. 2007; 128:171–182. [PubMed: 17218263]
16. Haling JR, Monkley SJ, Critchley DR, Petrich BG. Talin-dependent integrin activation is required for fibrin clot retraction by platelets. Blood. 2011; 117:1719–1722. [PubMed: 20971947]
17. Petrich BG, et al. Talin is required for integrin-mediated platelet function in hemostasis and thrombosis. Journal of Experimental Medicine. 2007; 204:3103–3111. [PubMed: 18086863]

18. Coller BS. Interaction of normal, thrombasthenic, and Bernard-Soulier platelets with immobilized fibrinogen: Defective platelet-fibrinogen interaction in thrombasthenia. Blood. 1980; 55:169–178. [PubMed: 6766334]
19. Ugarova TP, et al. Conformational changes in fibrinogen elicited by its interaction with platelet membrane glycoprotein GPIIb-IIIa. J Biol Chem. 1993; 268:21080–21087. [PubMed: 7691805]
20. Du X, et al. Ligands "activate" integrin alpha IIb beta 3 (platelet GPIIb-IIIa). Cell. 1991; 65:409–416. [PubMed: 2018974]
21. Arias-Salgado EG, Lizano S, Shattil SJ, Ginsberg MH. Specification of the direction of adhesive signaling by the integrin beta cytoplasmic domain. J Biol Chem. 2005; 280:29699–29707. [PubMed: 15937333]
22. Goksoy E, et al. Structural basis for the autoinhibition of talin in regulating integrin activation. Molecular Cell. 2008; 31:124–133. [PubMed: 18614051]
23. Xi XD, Bodnar RJ, Li ZY, Lam SCT, Du XP. Critical roles for the COOH-terminal NITY and RGT sequences of the integrin beta(3) cytoplasmic domain in inside-out and outside-in signaling. Journal of Cell Biology. 2003; 162:329–339. [PubMed: 12860973]
24. Krishnadas A, Rubinstein I, Onyuksel H. Sterically stabilized phospholipid mixed micelles: in vitro evaluation as a novel carrier for water-insoluble drugs. Pharm Res. 2003; 20:297–302. [PubMed: 12636171]
25. O'Brien KA, Gartner TK, Hay N, Du X. ADP-stimulated activation of Akt during integrin outside-in signaling promotes platelet spreading by inhibiting glycogen synthase kinase-3beta. Arteriosclerosis, thrombosis, and vascular biology. 2012; 32:2232–2240.
26. Delaney MK, Liu J, Zheng Y, Berndt MC, Du X. The role of Rac1 in glycoprotein Ib-IX-mediated signal transduction and integrin activation. Arteriosclerosis, thrombosis, and vascular biology. 2012; 32:2761–2768.
27. Cho J, et al. Protein disulfide isomerase capture during thrombus formation in vivo depends on the presence of beta3 integrins. Blood. 2012; 120:647–655. [PubMed: 22653978]
28. O'Brien KA, Stojanovic-Terpo A, Hay N, Du X. An important role for Akt3 in platelet activation and thrombosis. Blood. 2011; 118:4215–4223. [PubMed: 21821713]
29. Marjanovic JA, Li Z, Stojanovic A, Du X. Stimulatory roles of nitric-oxide synthase 3 and guanylyl cyclase in platelet activation. J Biol Chem. 2005; 280:37430–37438. [PubMed: 16144836]
30. Nimura N, Kinoshita T, Yoshida T, Uetake A, Nakai C. 1-Pyrenyldiazomethane as a fluorescent labeling reagent for liquid chromatographic determination of carboxylic acids. Analytical chemistry. 1988; 60:2067–2070. [PubMed: 3239787]

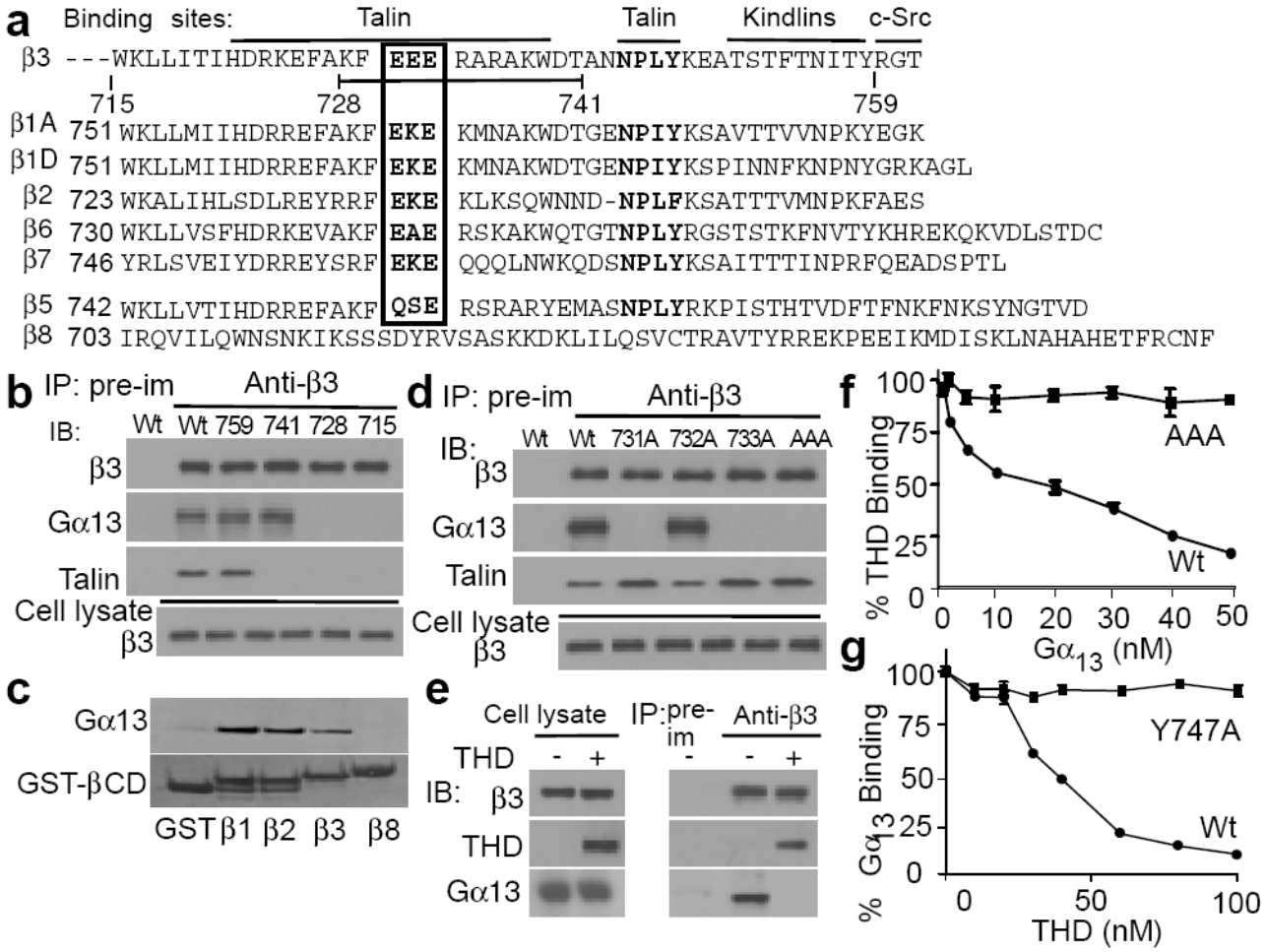

Fig. 1. Mutually exclusive binding of talin and $G\alpha_{13}$ to β_3

(a) The sequence of human β_3 cytoplasmic domain and its alignment with other β subunits showing conserved ExE motifs and binding sites for talin, kindlins and c-Src. **(b)** Co-immunoprecipitation of Wt and truncated mutant β_3 with $G\alpha_{13}$ and talin using anti-β_3 or control pre-immune rabbit serum. Immunoprecipitates and CHO cell lysates (10% of that used in immunoprecipitation) were immunoblotted (IB) with indicated antibodies. **(c)** Binding of purified recombinant $G\alpha_{13}$ to glutathione bead-bound glutathione S-transferase (GST), GST-β_1 cytoplasmic domain fusion protein (GST-β_1CD), GST-β_2CD, GST-β_3CD, or GST-β_8CD. **(d)** Coimmunoprecipitation of CHO cell-expressed Wt or ExE motif mutated β_3 with $G\alpha_{13}$ and talin using anti-β_3 or pre-immune rabbit serum. **(e)** Coimmunoprecipitation of CHO cell-expressed integrin $\alpha_{IIb}\beta_3$ with $G\alpha_{13}$ and THD following transfection with cDNA encoding THD. **(f, g)** Inhibition of the binding of THD (20 nM) **(f)** or $G\alpha_{13}$ (40 nM) **(g)** to immobilized GST-β_3CD proteins (Wt and negative control mutants) by increasing concentrations of $G\alpha_{13}$ **(f)** or THD **(g)**. Bound $G\alpha_{13}$ or THD was detected using anti-$G\alpha_{13}$ or anti-talin.

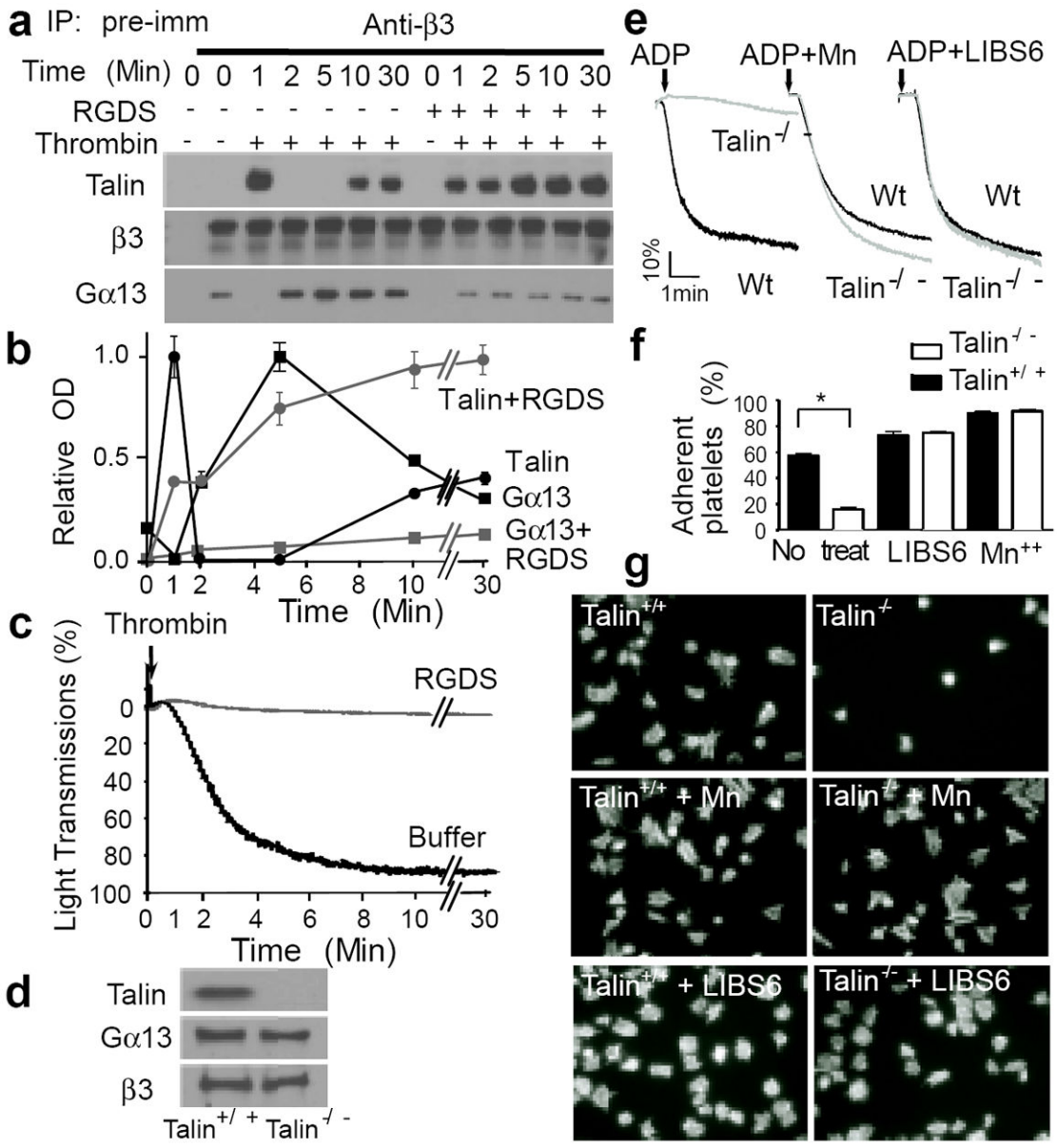

Fig. 2. Dynamics of talin and $G\alpha_{13}$ binding to β_3 and the role of talin in integrin signaling

(a, b and c) Human platelets were stimulated with 0.025 U/ml α-thrombin (in an aggregometer) with or without 2 mM integrin inhibitor RGDS, solubilized at various time points, immunoprecipitated with anti-β_3 or pre-immune rabbit serum, and immunoblotted for $G\alpha_{13}$, talin, and β_3 (additional controls in E.D. Fig 3d). **(a)** Typical immunoblots. **(b)** Quantification of immunoblots (mean ± SD, 3 experiments). **(c)** Turbidity changes indicating integrin-dependent platelet aggregation. **(d)** Immunoblotting of talin-1 in Wt and talin-$1^{-/-}$ mouse platelets. **(e)** Aggregation of Wt and talin-$1^{-/-}$ platelets stimulated with 5 μM ADP in the presence of 20μg/ml fibrinogen, with or without 1 mM $MnCl_2$ or 0.3μg/ml LIBS6. **(f)** Adhesion of unstimulated mouse platelets to immobilized fibrinogen for 1 hour, with or without 1 mM $MnCl_2$ or 0.18μg/ml LIBS6 (quantified as percentage of loaded platelets, mean ± SD, n=4, *p<0.001). **(g)** Images of phalloidin-stained mouse platelets

spreading on fibrinogen for 1 hour, with or without 1 mM $MnCl_2$ or 0.18μg/ml LIBS6 (quantification in E.D. Fig 4e).

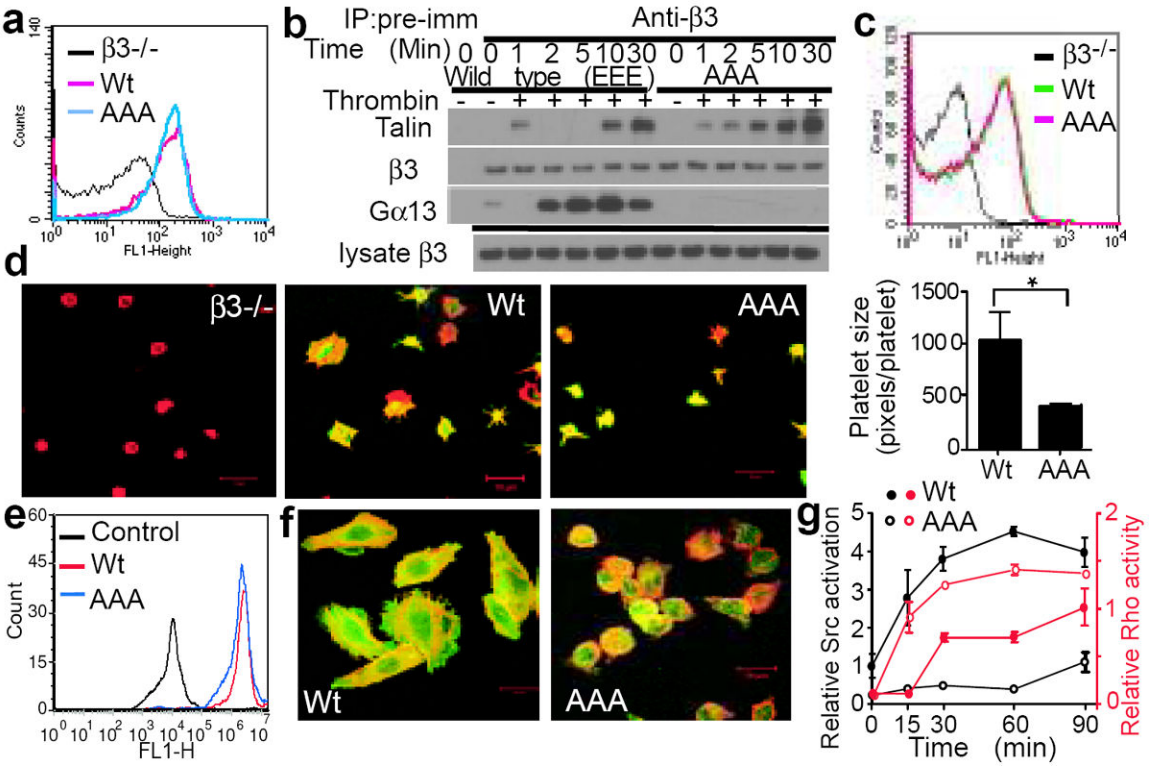

Fig. 3. The selective role of Gα$_{13}$-ExE binding in integrin outside-in signaling

(a) Flow cytometric analysis of β_3 expression in platelets from $\beta_3^{-/-}$ mice transplanted with Wt or AAA-mutant β_3-transfected bone marrow stem cells. $\beta_3^{-/-}$ platelets served as negative control. **(b)** Mouse platelets expressing Wt or AAA mutant β_3 were stimulated with 0.025 U/ml α-thrombin, solubilized at various time points, immunoprecipitated with anti-β_3 or pre-immune rabbit serum, and immunoblotted for Gα_{13}, talin, and β_3. **(c)** PAR4AP-induced binding of Oregon-Green-labelled fibrinogen to Wt or AAA-mutant $\alpha_{IIb}\beta_3$-expressing platelets with $\beta_3^{-/-}$ platelets as a negative control. **(d)** Confocal images of $\beta_3^{-/-}$ platelets and $\beta_3^{-/-}$ platelets expressing Wt or AAA-mutant β_3 spreading on fibrinogen and surface area quantification (mean ± SE). Merged anti-β_3 (green) and Alexa Fluor 546-conjugated phalloidin (red) fluorescence. **(e)** Flow cytometric analysis of Wt or β_3 E731-733A (AAA) mutant $\alpha_{IIb}\beta_3$ expression in CHO-1b9 cells. **(f)** Confocal images of phalloidin (red)/ anti-β_3 (green)-double stained Wt and AAA-mutant $\alpha_{IIb}\beta_3$-expressing CHO cell spreading on fibrinogen (45min). **(g)** RhoA activation and c-Src Tyr416 phosphorylation in Wt or AAA-mutant $\alpha_{IIb}\beta_3$-expressing CHO-1b9 cells adherent to fibrinogen (mean ± SD, n=3).

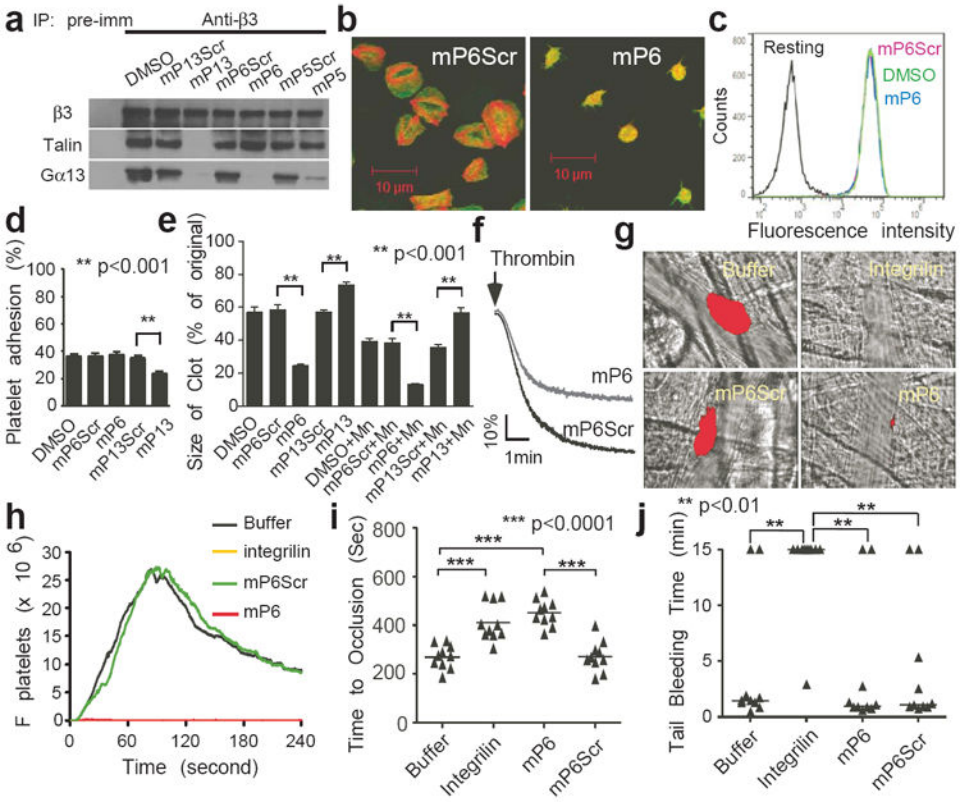

Fig. 4. A new anti-thrombotic that does not cause bleeding

(a) The effects of 500 μM mP_{13}, mP_6, or mP_5 on co-immunoprecipitation of β_3 with $G\alpha_{13}$ or talin in thrombin-stimulated platelets in comparison with scrambled controls (also see E.D. Fig 7). **(b)** Confocal images of phalloidin (red)/anti-β_3 (green)-double-stained human platelets treated with 100 μM mP_6 or mP_6Scr spreading on immobilized fibrinogen (1 hour). **(c)** PAR4AP-induced Oregon-Green-labelled fibrinogen binding to human platelets pre-treated with DMSO or 100 μM mP_6Scr or mP_6. **(d)** Effect of mP_6 and mP_{13} (250 μM) on resting platelet adhesion to immobilized fibrinogen as compared with scrambled peptides (mean ± SD, n=4). **(e)** Effect of mP_6 or mP_{13} (250 μM) on clot retraction of human platelet-rich plasma, with or without 1 mM manganese (mean ± SD, n=3). **(f)** Effects of 10 μM mP_6 or mP_6Scr micelles on platelet aggregation induced by 0.03 U/ml thrombin. **(g)** Comparison of mP_6 micelle (5 μmol/kg) with Integrilin (12 μmol/kg) and their respective controls in inhibiting laser-induced arteriolar thrombosis in mice. Representative images at 60 seconds after injury are shown. Platelet thrombi were indicated by DyLight 649-labelled nonblocking rat anti-mouse GPIbβ (red). **(h)** Quantification of (g). The median integrated platelet fluorescence ($F_{platelets}$) during thrombosis at 30 injury sites in 3 mice. **(i)** Comparison of mP_6 (5 μmol/kg) with Integrilin (5 μmol/kg) and their respective controls in inhibiting $FeCl_3$-induced carotid artery thrombosis in mice. **(j)** Comparison of mP_6 (5 μmol/kg) with Integrilin (5 μmol/kg) and controls in mouse tail bleeding time analysis.